

Hectogram-scale Green Synthesis of Hierarchical 4A Zeolite @

$\text{CuO}_x(\text{OH})_{(2-2x)}(0 \leq x < 1)$ Nanosheet Assemblies Core-Shell

Nanoarchitectures with Superb Congo Red Adsorption Performance

Leitao Zhang^{a,b,§}, Lilan Huang^{a,§}, Lei Zhang^a, Binzhong Lu^b, Junbo Li^b, Yingfang Xie^a, Qiang Ma^a, Qingping Xin^a, Hui Ye^a, Lizhi Zhao^a, Yuzhong Zhang^{a,□}, Hong Li^a.

§ These authors contributed equally to this work and were the co-first authors;

□ Corresponding author: Yuzhong Zhang

Corresponding E-mail: Zhangyz2004cn@163.com

a State Key Laboratory of Separation Membranes and Membrane Processes, School of Materials Science and Engineering, Tianjin Polytechnic University, Tianjin 300387, PR China

b School of Chemical Engineering and Pharmaceutics, Henan University of Science and Technology, Luoyang 47100, Henan, P. R. China.

S1 Characterizations of as-obtained adsorbents

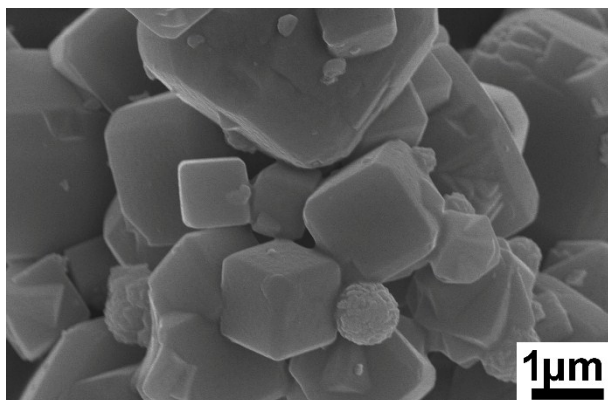


Figure S1. The SEM image of 4A zeolite.

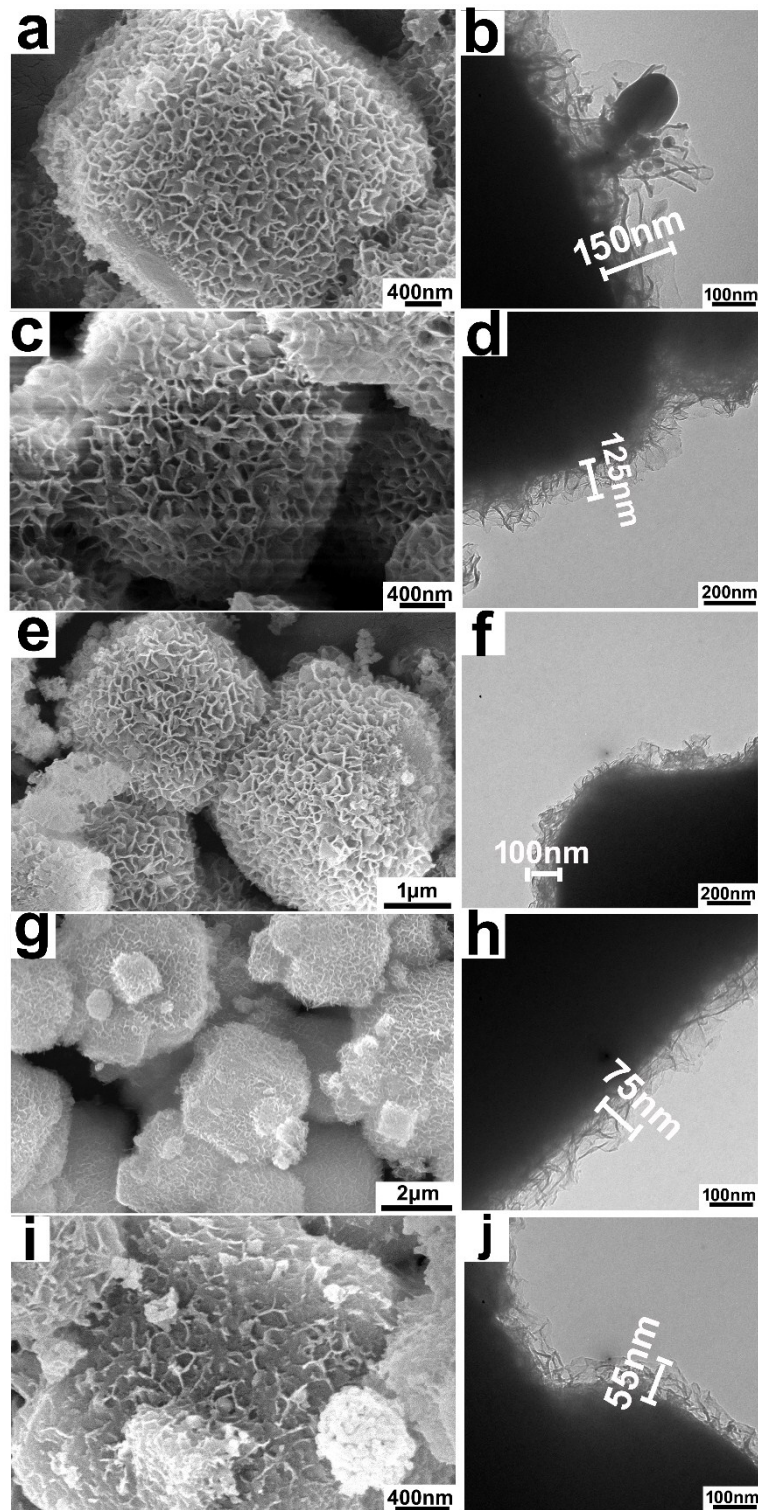


Figure S2. The effect of temperature treatment on the thickness of $\text{CuO}_x\text{Cu}(\text{OH})_{(2-2x)}$ ($0 \leq x < 1$) nanosheet assemblies on the surface of 4A zeolite. **SEM images:** a) 4A-Cu (-55°C); c) 4A-Cu-200 (200°C); e) 4A-Cu-300 (300°C); g) 4A-Cu-400 (400°C); i) 4A-Cu-500 (500°C). **TEM images:** b) 4A-Cu (-55°C); d) 4A-Cu-200 (200°C); f) 4A-Cu-300 (300°C); h) 4A-Cu-400 (400°C); j) 4A-Cu-500 (500°C).

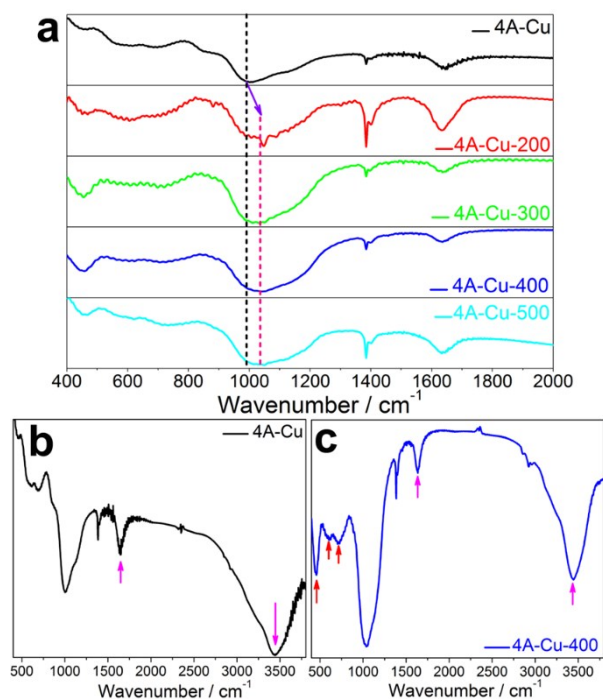


Figure S3. The FTIR of core-shell 3D assemblies. a) The FTIR fingerprint of 4A-Cu, 4A-Cu-200, 4A-Cu-300, 4A-Cu-400 and 4A-Cu-500. The FTIR spectra range from 400cm-1 to 4000cm-1 of (b) 4A-Cu and (c) 4A-Cu-400.

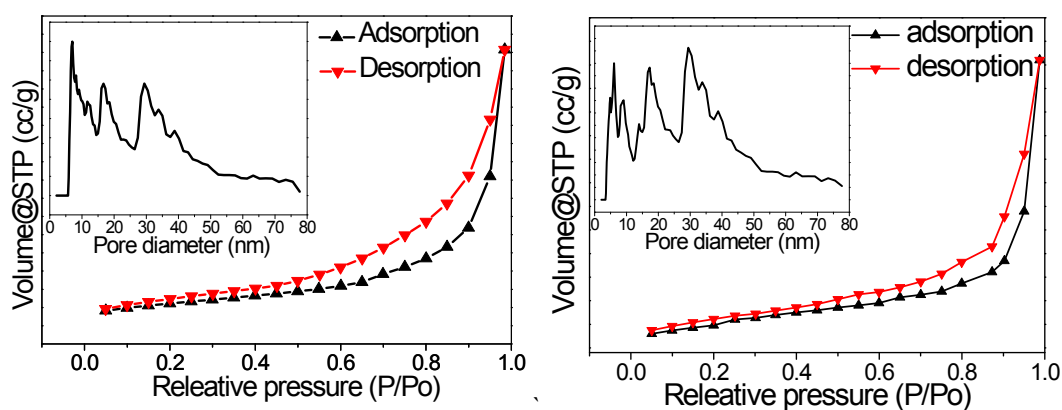


Figure S4. N₂ adsorption / desorption isotherms and pore size distribution (inset) of left) 4A-Cu and right) 4A-Cu-300.

Table S1. The physical properties of 4A zeolite, 4A-Cu and 4A-Cu-T samples.

Sample	4A-Cu	4A-Cu-200	4A-Cu-300	4A-Cu-400	4A-Cu-500	4A zeolite
Specific surface area(m ² g ⁻¹) ^a	18.621	19.287	18.020	9.591	7.192	573 ^b
Mean pore size (nm) ^a	7.032	10.681	29.396	17.296	2.769	0.4 ^b

Note: ^aCalculated using the NLDFT method. ^bObtained based on the literature¹.

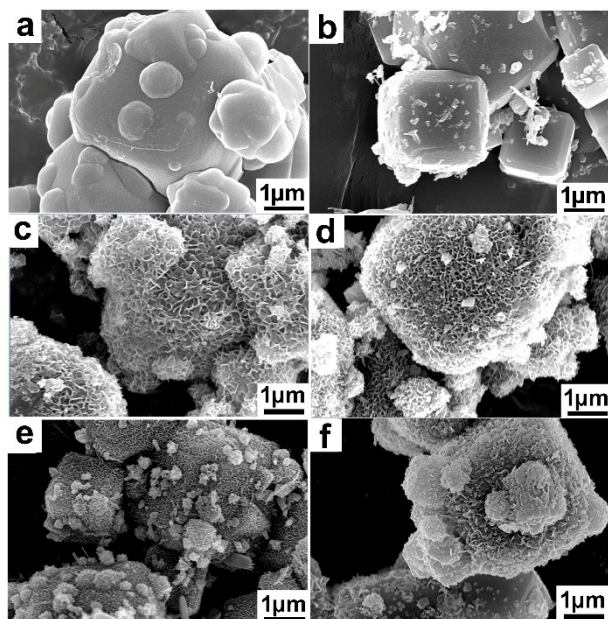
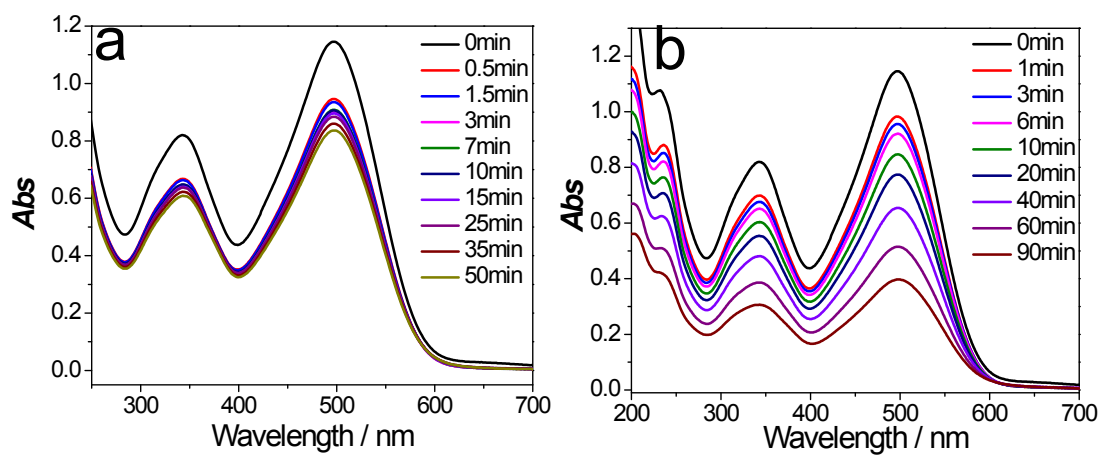


Figure S5. The pH effects on the surface morphology of 4A zeolite@CuO_xCu(OH)_(2-2x) (0 ≤ x < 1) nanosheet assemblies core-shell hierarchical architectures: a) pH=1.20; b) pH=1.40; c) pH=1.60; d) pH=1.80; e) pH=2.00; f) pH=4.18.

S2 Adsorption experiments of Congo red dye



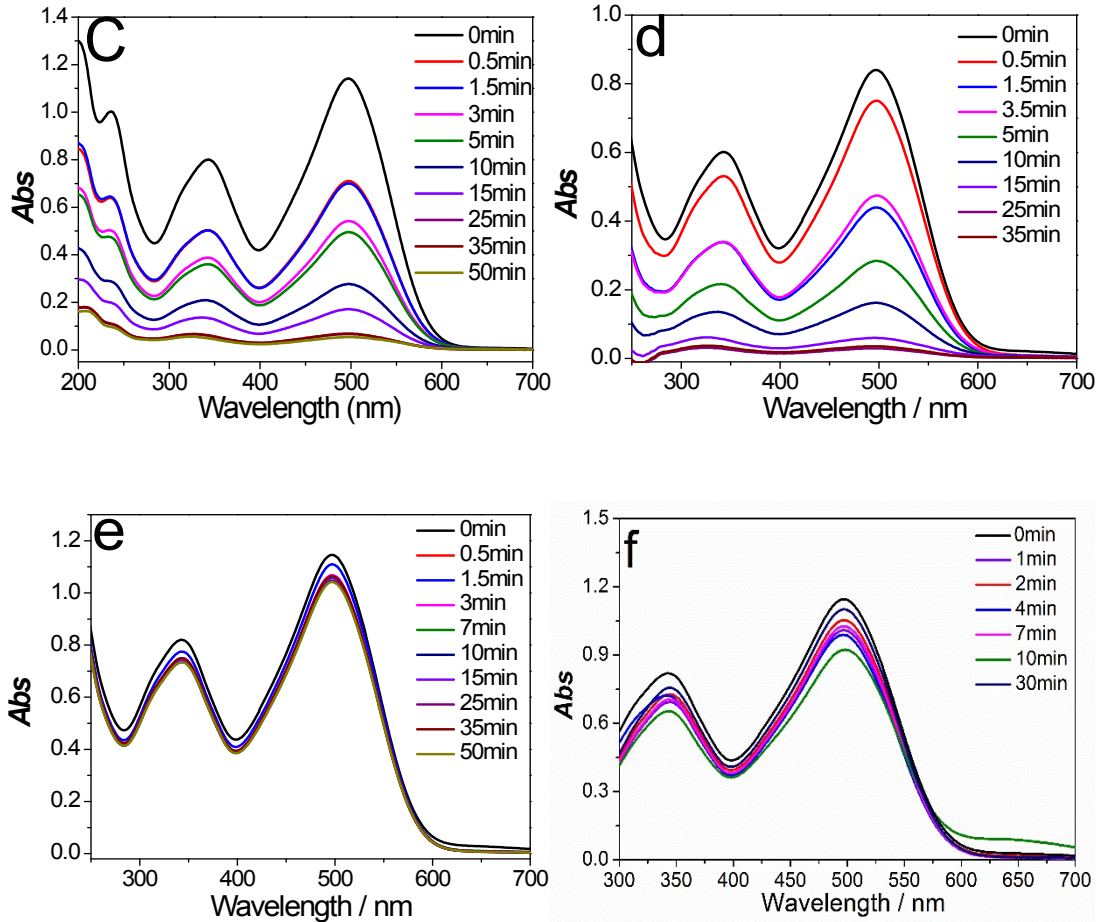


Figure S6. The time dependence of the concentration of Congo Red dye with different as-prepared adsorbents: a) 4A-Cu, b) 4A-Cu-200, c) 4A-Cu-300, d) 4A-Cu-400, e) 4A-Cu-500 and f) 4A-Cu-900. Other conditions: Congo Red=100 ml, 1000 mg/L (CR concentration in 4A-Cu-900 adsorption study is 100 mg/L); adsorbent=0.2 g; pH=6.30; T=25^oC.

S3 The fitting model for Congo red adsorption experiments

The pseudo-first-order kinetic model (Eq.1) and pseudo-second-order kinetic model (Eq.2) are represented as followed to describe the Congo Red removal on 4A zeolite @ CuO_x(OH)_(2-2x)(0≤x<1) hierarchical architectures.

$$\ln(q_e - q_t) = \ln q_e - \frac{k_1 t}{2.303} \dots \dots \dots \text{Eq.1}$$

$$\frac{t}{q_t} = \frac{1}{k_2 q_e^2} + \frac{t}{q_e} \dots \dots \dots \text{Eq.2}$$

where q_e and q_t are adsorption capacity at equilibrium and at any time t (min), respectively. k₁ (min⁻¹) and k₂ (g·mg⁻¹·min⁻¹) are the pseudo-first-order and pseudo-second-order rate constants.

The Langmuir (Eq.3) and Freundlich (Eq.4) models were applied to study the adsorption mechanism of Congo Red on the surface of 4A-Cu-300.

$$q_e = \frac{q_m b C_e}{1 + b C_e} \dots \dots \dots Eq.3$$

$$q_e = k_f C_e^{1/n} \dots \dots \dots Eq.4$$

In Eq.3, q_m (mg/g) is the maximum adsorption capacity corresponding to complete monolayer coverage, and the b is the equilibrium constant (L/mg). While K_f is an indicator of the adsorption capacity, and n is the adsorption intensity.

Table S2 The kinetic-fitting results of Congo Red adsorption experiments.

Sample	Pseudo-first-order-kinetic model			Pseudo-Second-order-kinetic model		
	R ²	k_1 (min ⁻¹)	q_e (mg/g)	R ²	k_2 (g·mg ⁻¹ ·min ⁻¹)	q_e (mg/g)
4A zeolite	0.852	1.1967	4.663	0.880	0.0011	4.896
4A-Cu	0.943	1.1001	172.140	0.974	0.6236	182.537
4A-Cu-200	0.960	0.0525	309.532	0.977	18.1240	379.445
4A-Cu-300	0.971	0.2911	463.572	0.994	2.3615	508.379
4A-Cu-400	0.967	0.7657	459.210	0.994	0.9765	495.488
4A-Cu-500	0.942	1.0807	39.360	0.954	0.0183	41.805
4A-Cu-900	0.934	0.1885	9.095	0.974	0.0107	10.604

Note: The kinetic-fitting study of 4A zeolite and 4A-Cu-900 was executed with the concentration of Congo Red being 100mg/L. Other fitting calculations was carried out when the concentration of Congo Red was 100mg/L.

Table S3. The fitting results of isothermal adsorption experiments with 4A-Cu-300 adsorbents.

Sample	Langmuir model			Freundlich model		
	R ²	K_L (L/mg)	q_e (mg/g)	R ²	K_f ((mg/g)·(L/mg) ^{1/n})	n
4A-Cu-300	0.959	8.48749	512.987	0.879	137.61718	4.632

S4 The calculation method of adsorption capacity

The weight ratio of copper elements is 9.09%, and the maximum adsorption capacity of 4A-Cu-300 is 512.987mg/g. Three standards are taken into consideration to calculate the maximum adsorption capacity.

1 If we use the copper as the standard criteria to calculate the adsorption capacity, the maximum

capacity is $\frac{512.987mg/g}{9.09\%} = 5643.421mg/g$;

2 If the CuO is used as the criteria, the maximum capacity is

$\frac{512.987mg/g}{9.09\%} \times \frac{64}{80} = 4514.737mg/g$;

3 If the Cu(OH)₂ is applied to calculate the capacity, the maximum adsorption capacity is

$$\frac{512.987\text{mg}}{\text{g}} \div 9.09\% \times \frac{64}{98} = 3685.500\text{mg/g}.$$

In fact, given that the CuO and Cu(OH)₂ phase coexist in the shell structure of 4A-Cu-300, the lowest limit of the maximum adsorption capacity is 3685.500mg/g.

REFERENCES

- (1) Zhang, L.; Ye, H.; Zhao, L.; Zhang, L.; Yao, L.; Zhang, Y.; Li, H. Design of isolated iron species for Fenton reactions: lyophilization beats calcination treatment. *Chem. Commun.* **2015**, *51*, 16936-16939.